

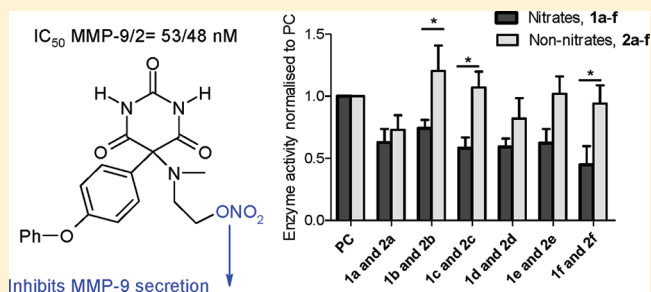
## Design of Barbiturate–Nitrate Hybrids that Inhibit MMP-9 Activity and Secretion

Jun Wang, Shane O’Sullivan, Shona Harmon, Ray Keaveny, Marek W. Radomski, Carlos Medina, and John F. Gilmer\*

School of Pharmacy and Pharmaceutical Sciences, Trinity College, Dublin 2, Ireland

**S** Supporting Information

**ABSTRACT:** We describe a new type of barbiturate-based matrix metalloproteinase (MMP) inhibitor incorporating a nitric oxide (NO) donor/mimetic group (series 1). The compounds were designed to inhibit MMP at enzyme level and to attenuate MMP-9 secretion arising from inflammatory signaling. To detect effects related to the nitrate, we prepared and studied an analogous series of barbiturate C5-alkyl alcohols that were unable to release NO (series 2). Both series inhibited recombinant human MMP-2/9 activity with nanomolar potency. Series 1 consistently inhibited the secretion of MMP-9 from TNF $\alpha$ /IL1 $\beta$  stimulated Caco-2 cells at 10  $\mu$ M, which could be attributed to NO related effects because the non-nitrate panel did not affect enzyme levels. Several compounds from series 1 (10  $\mu$ M) inhibited tumor cell invasion but none from the non-nitrate panel did. The work shows that MMP-inhibitory barbiturates are suitable scaffolds for hybrid design, targeting additional facets of MMP pathophysiology, with potential to improve risk-benefit ratios.



### INTRODUCTION

The matrix metalloproteinase (MMP) enzymes and their tissue inhibitors contribute to the regulation of the extracellular matrix and processing of myriad endogenous substances.<sup>1,2</sup> Members of the human MMP gene family (24) are classified according to function and substrate specificity.<sup>3</sup> Gelatinases A (MMP-2, EC 3.4.24.24) and B (MMP-9, EC 3.4.24.35) contain fibronectin-like inserts, enabling them to bind and process gelatin. The gelatinases degrade collagen type IV assisting cellular migration processes<sup>4</sup> that are relevant to the pathogenesis of cancer, heart disease, and inflammation.<sup>5–8</sup> MMP-9 is also linked with cancer because this stromal-derived enzyme can promote tumor angiogenesis. However, even in disease states, the gelatinases continue to perform physiological functions, some of which oppose the pathophysiology.<sup>9</sup> Progress in the gelatinase inhibitor field may therefore require approaches that can target aberrantly regulated enzyme.

The promoter region of the MMP-9 gene contains cis-acting regulatory elements with binding sites for NF $\kappa$ B, AP-1, and PEA-3.<sup>10–13</sup> MMP-9 expression is therefore responsive to various cytokines including IL-1 $\beta$ , IL-2, IL-8, TNF- $\alpha$ , growth factors, lipopolysaccharide, and phorbol esters.<sup>14,15</sup> Endogenous and pharmacologically derived nitric oxide (NO) is reported to interact with these signaling pathways, leading in several reported cases to inhibition of MMP-9 transcription/secretion. For example, S-nitrosylation of its p50 subunit (NO<sup>+</sup>) has been shown to reduce NF $\kappa$ B-binding in multiple cell lines.<sup>16,17</sup> Incubation with the NO donor DETA-NO leads to reduced AP1 binding, while inhibition of inducible NO synthase

increased IL-1 $\beta$  mediated AP1 activation.<sup>17,18</sup> At another level, NO is reported to destabilize MMP-9 mRNA, leading to reduced enzyme levels.<sup>19</sup> There are, on the other hand, some reports of NO activation of MMP activity.<sup>20</sup> High levels of NO and its byproduct can catalyze oxidation of the inhibitory cysteine on its prodomain causing activation of proMMP-9.<sup>16,21</sup> The interplay between NO and MMP-9 is evidently complex. An MMP-inhibitory NO donor hybrid might be useful for investigating this relationship, and it could have clinical potential in pathological situations where inducible MMP-9 plays a significant role. NO-donating or NO-mimetic hybrids have been designed for diverse drug types<sup>22–24</sup> (particularly in the anti-inflammatory field), leading in several instances to clinical candidates with improved risk–benefit profiles.<sup>25</sup> Usually, the NO-donating group abrogates activity and the hybrid acts as a prodrug of the two moieties.<sup>23</sup> However, the topological features of the MMP-9 catalytic site suggested that it might be possible to incorporate an NO-donor group into an established MMP-inhibitor type without sacrificing enzyme affinity.

C-5 disubstituted pyrimidine-2,4,6-triones (barbiturates) are a relatively recently discovered MMP inhibitor drug-type with attractive PK/PD properties (Figure 1A).<sup>26–29</sup> Several high resolution structures reveal a mode of binding for compounds in this class that is similar to the more common hydroxamate inhibitor type. The enolized barbiturate ring binds the Zn atom

Received: October 9, 2011

Published: January 16, 2012

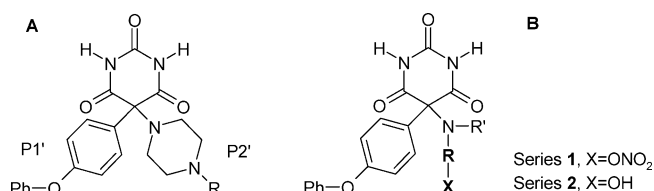


**Figure 1.** (A) C-5 piperazinyl barbiturates. (B) NO mimetic design series 1 and parallel alcohol series 2. P1', P2' denote the Schechter and Berger nomenclature for the pseudosubstrate positions occupied by these groups on binding MMP-9

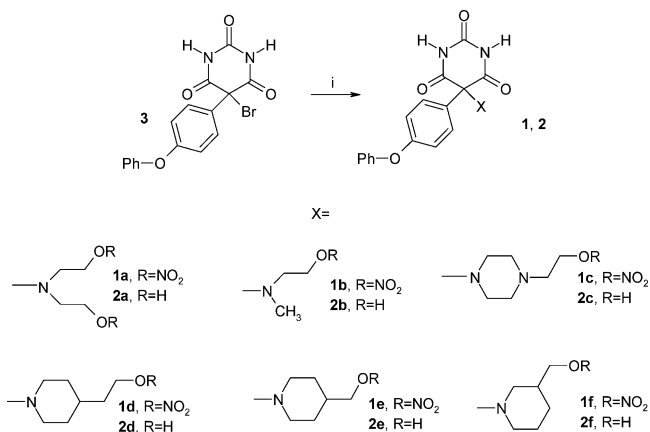
with one C-5 hydrophobic substituent occupying the deep S1' pocket. The geminal C5' group is directed toward the S2' pocket, the outer rim of which is solvent exposed.<sup>30</sup> These observations suggested that an NO mimetic group such as an organic nitrate could be placed at the terminus of either of the C-5 substituents without significantly affecting binding.

In this study, we have prepared a panel of C-5 aminoalkyl nitrates and the corresponding alcohols for comparison (Figure 1B). These were designed so that the C-5 phenyloxyphenyl group would occupy the S1' pocket with the alkyl nitrate group directed into the S2' pocket toward the solvent interface. We provide evidence that the nitrates possess intrinsic MMP-9 inhibitory activity, interfere with cancer cell invasion, release nitrite, and suppress tumor cell secretion of MMP-9.

## ■ SYNTHESIS AND EVALUATION OF GELATINASE INHIBITORS

The key intermediate to generate series 1 was the barbiturate-5-bromide **3** (Scheme 1). This is available in four steps from

### Scheme 1. Preparation of 5-Phenyloxyphenyl Barbiturate-5-aminoalkyl Nitrates (**1a–f**) and Aminoalkylalcohols (**2a–f**)<sup>a</sup>



<sup>a</sup>(i) aminoalkyl nitrates or corresponding aminoalcohols, Et<sub>3</sub>N, MeOH, RT, 24 h.

methyl 4-hydroxyphenylacetate as previously described.<sup>27</sup> The preparation of series 1 was achieved by allowing **3** to react with various aminoalkyl nitrates in the presence of triethylamine and MeOH at RT for 24 h (Scheme 1). The aminoalkyl nitrates were themselves obtained by reacting the corresponding commercially available aminoalkyl alcohols with fuming nitric acid at  $-10\text{ }^{\circ}\text{C}$ , over 20 min followed by addition of acetic anhydride.<sup>31</sup> The basic forms of the amines were isolated by extraction of basic solutions of nitrate salts with ethyl acetate and evaporation of the solvent. The aminoalkyl moieties were

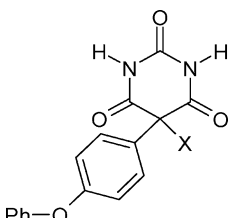
selected in order to produce three amino-ethyl nitrates (**1a–c**), as well as nitrates with greater separation between amino-nitrogen and nitrate (**1d–f**). A parallel series of aminoalkyl alcohol barbiturates (**2**) was independently produced by reacting **3** with the corresponding aminoalkyl alcohols in order to provide test compounds to isolate the contribution of the nitrate group to inhibition of gelatinase secretion. The identity and purity of the nitrates (series 1) and alcohols (series 2) was confirmed by IR, NMR, HPLC, and HRMS.

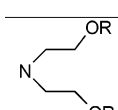
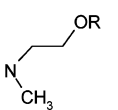
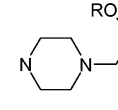
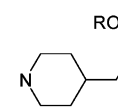
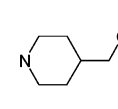
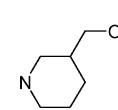
The inhibitory effects of series 1 and 2 on MMP-2 and MMP-9 was measured using a fluorogenic substrate assay with human recombinant MMP-2 and MMP-9. The compounds were tested at 0.01–10000 nM following incubation for 45 min.

In general, the non-nitrate series 2 were more potent inhibitors of MMP-2 and -9 than series 1 (Table 1). This disparity was marked in the case of **2a**, which was 86-fold more potent for MMP-2 and 3.5-fold over MMP-9 than its nitrate analogue **1a**. The high potency of **2a** against MMP-2 was a somewhat surprising. However, the relatively high potency of compounds in series 1 and 2 featuring piperazine or piperidines is consistent with the literature on MMP inhibitory barbiturates.<sup>26–30</sup> Among the nitrates, **1b** (IC<sub>50</sub>: MMP-2 = 53.05 nM, MMP-9 = 47.58 nM) was the most potent inhibitor of both MMP-2 and MMP-9; indeed it departed from the general pattern in being more potent against MMP-9 than its non-nitrate analogue (**2b**). Another interesting nitrate, **1a** exhibited 3-fold selectivity for MMP-9 over MMP-2. The short incubation time and test medium allow us to exclude any contribution of nitrate activation to these results.

It was interesting to investigate the disposition of the nitrate groups of series 1 on binding MMP-9, with the barbiturate and 5-phenyloxyphenyl group in their predicted orientations. Figure 2a shows representative conformations following docking experiments (AutoDock 4) with **1a** using the X-ray crystal structure of a mutant MMP-9 bound to a 5-piperazinyl barbiturate (PDB code 2OVX).<sup>30</sup> Figure 2b shows a low energy docking pose for **1c** overlain with the piperazinyl ligand in PDB 2OVX. The aminoalkyl nitrate groups of **1a** and **1c** are directed through the S2' pocket toward the enzyme surface. The nitrate groups would be solvent exposed in this pose. The greater potency of the aminoalkyl alcohols may be due to their ability to form H-bonds with water and solvent surface. In contrast, binding of series 1 in the high affinity mode places the relatively lipophilic nitrate ester in a thermodynamically unfavorable solvent exposed position. There is clearly scope for enhancing potency in the nitrate-substituted class, possibly by increasing polarity in the side chain or by moving the nitrate further from the catalytic site. We did not try to improve potency in this study because it was felt that the characteristics of **1a–f** represented an interesting balance of potential to donate or mimic NO as well as gelatinase inhibitory potency. The inhibitory data and docking analysis reinforce the idea that barbiturate-based compounds could not only act as gelatinase inhibitors by binding to MMP-2 and MMP-9, but scaffolds for hybrid compounds possessing other pharmacological actions or indeed NO-donating moieties such as furox(az)ans and diazeniumdiolates.<sup>32</sup>

MMPs can promote cancer cell invasion by degradation of various extracellular matrix components resulting in release of growth factor and cytokines. Inhibition of MMP activity, especially MMP-9, has the potential to inhibit tumor growth and metastasis.<sup>6</sup> In addition, NO donors have been reported to inhibit cell proliferation and invasion, including pancreatic,

Table 1. IC<sub>50</sub> Values (nM) for Inhibition of Recombinant Human Gelatinases (95% CI)<sup>a</sup>


X=	R=	IC <sub>50</sub> (nM)			R=	IC <sub>50</sub> (nM)		
		MMP-2	MMP-9	% I		MMP-2	MMP-9	% I
	NO <sub>2</sub>				H			
	<b>1a</b>	328 (273–395)	91 (63–131)	51.4 ±2.8	<b>2a</b>	3.8 (2.6–5.7)	26 (21–32)	51.2 ±8.6
	<b>1b</b>	53 (43–65)	48 (38–60)	44.6 ±4.8	<b>2b</b>	24 (15–36)	145 (110–191)	34.4 ±8.1
	<b>1c</b>	149 (129–171)	92 (71–118)	34.8 ±7.4	<b>2c</b>	7.3 (5.3–9.9)	8.1 (7–10)	46.3 ±9.3
	<b>1d</b>	158 (125–199)	152 (120–193)	nd	<b>2d</b>	10 (7.5–14)	12 (7.7–19)	nd
	<b>1d</b>	219 (174–274)	212 (170–266)	35.8 ±12.3	<b>2e</b>	66 (51–86)	97 (81–115)	39.0 ±7.0
	<b>1f</b>	179 (155–208)	104 (77–140)	40.7 ±6.2	<b>2f</b>	15 (9–26)	6.2 (4–9)	55.3 ±3.8

<sup>a</sup>The %I values represent the % reduction in the number of Caco-2 cells migrating across a matrigel membrane in response to stimulation with HGF (100 ng/mL) in the presence of test compounds at 100 nM (±sd,  $n = 3 \times 2$ ).

prostate, and bladder cancer cells.<sup>33</sup> Furthermore, NO can inhibit the release of gelatinases from cancer cells. Therefore we compared the effect of series 1 and 2 (100 nM) on cell migration using an in vitro model of cancer cell invasiveness. In this model, Caco-2 cells migrate through a matrigel membrane following stimulation with hepatocyte growth factor (HGF, 100 ng/mL) (%I in Table 1). Relative amounts of cells on each side of the membrane were counted by microscope following staining. Both sets of compounds inhibited cell migration but not in a manner that could be related to potency, gelatinase selectivity, or ability to donate NO.

Because we had conducted a number of assays with the compounds assessing biochemical effects that might be attributable to NO related-effects, it was timely to make some evaluation of their ability to undergo nitrate metabolism in a cellular environment.

Nitrate esters were selected for the present study because of their ease of preparation, good stability, and relative lipophilicity. Moreover, alkyl nitrates remain in widespread clinical use despite concerns about tolerance or endothelial dysfunction

and the emergence of other NO donor types. Nitrate esters are activated by mitochondrial aldehyde reductase-2 and by smooth muscle cell P450 enzymes in a manner that is substrate structure dependent.<sup>34</sup> Indeed, the consequences of nitrate metabolism and downstream effects are substrate and concentration dependent.<sup>35,36</sup> Nitrite and nitrate are prominent metabolic byproducts and intermediates of these processes.<sup>37,38</sup> Indeed, the NO donor/mimetic effects of organic nitrates may be mediated via nitrite.<sup>34</sup> We used a modified Griess assay to measure the ability of the **1a–f** to release nitrite/nitrate (cumulatively NO<sub>x</sub>).<sup>39</sup> In initial studies, we found that the extent of NO<sub>x</sub> release was influenced by cell density. The nitrate compounds **1a–f** were incubated in the presence of Caco-2 cells for 24 h at 200 and 10 μM (Table 2). A high level of NO<sub>x</sub> was detected in the supernatants of cells treated with the aminoethyl nitrate compounds **1a–c** at 200 μM. This was present as nitrite with **1a–b** and nitrate in the case of **1c**. At 10 μM, there were no apparent differences between the compounds in capacity to generate NO<sub>x</sub> species, suggesting a saturable metabolism pathway for the piperidine nitrates **1e–f**.



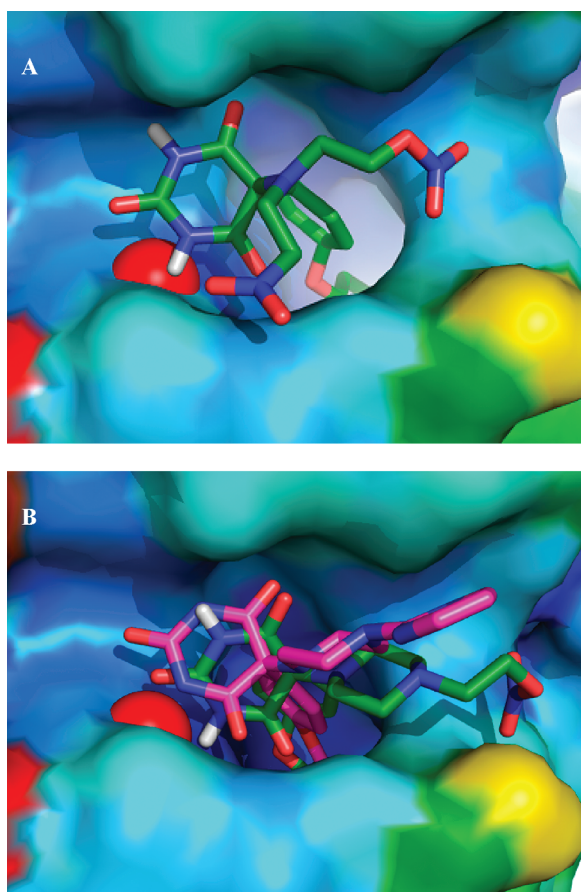


**Figure 2.** Connolly surface on MMP-9 generated by the program PyMOL based on the crystal structures of MMP-9 (PDB code 2OVX). The ligand orientations of **1a** (A) and **1c** (B) had the lowest binding energy of the conformations fitted into the designated pocket of the MMP-9, calculated using Autodock4 based on the 100 runs in the crystal structure of the MMP-9 (2OVX). The orientation of the overlaid ligand 5-(4-phenoxyphenyl)-5-(4-pyrimidine-2-ylpiperazin-1-yl)-pyrimidine-2,4,6-trione was directly taken from the mutant MMP-9 crystal structure file (2OVX).<sup>30</sup> The surfaces were generated by the programme PyMOL based on the crystal structures of MMP-9 (PDB code 2VOX). Ligand orientations were used which had the lowest binding energy of the conformations of 50 runs with 25000000 energy evaluations in Autodock4 and displayed by PyMOL. The active site Zn atoms appear as red spheres.

The impact of the hybrid compounds (100  $\mu\text{M}$ ) on gelatinase secretion, a key proof-of-concept assay, was performed using HT1080 fibrocarcinoma cells stimulated with phorbolmyristate acetate (PMA, 10  $\mu\text{M}$ ). The flasks were incubated at 5%  $\text{CO}_2$ , 37  $^\circ\text{C}$  for 24 h, after which time the supernatants were collected. Supernatants from the treated cells were loaded onto a zymography gel at constant protein concentration and MMP-2 and MMP-9 separated electro-

phoretically. Then the gel was washed and incubated for 48 h to allow gelatinolytic digestion to occur. The MMP-2 and MMP-9 activities of the resulting bands, as reflected in densitometry values, provides an index of enzyme activity. We separately showed with test inhibitors, and with the broad spectrum MMP inhibitor phenanthroline, that under these conditions, the density of the enzyme spot was unaffected by the inhibitor which dissociates from the enzyme during separation and becomes diluted to below its  $\text{IC}_{50}$ . MMP-2 and MMP-9 were highly expressed in PMA (10  $\mu\text{M}$ ) treated HT1080 cells. At 100  $\mu\text{M}$ , compounds **1a**, **1c**, and **1e–f** inhibited MMP-9 secretion by >80%. The compounds also inhibited MMP-2 expression, albeit to a lesser extent. Compounds **1b** and **1d** caused modest inhibition of secretion of both enzymes. Because MMP-2 is a housekeeping enzyme under indirect transcriptional control (mainly through MTP-1/MMP14<sup>40</sup>), we suspected that the apparently impressive effects on MMP production could be partially due to effects on cell viability in addition to dampening of pro-inflammatory signaling. Therefore we evaluated the effect of series 1 and 2 on cell viability using the 3-(4,5-dimethylthiazol-2-yl)-2,5-diphenyltetrazolium bromide assay (MTT) (Table 3). Several compounds from both series exhibited low micromolar  $\text{IC}_{50}$  values for reducing cell viability. Various chemically unrelated MMP inhibitors (e.g., hydroxamates) have been reported to possess high cytotoxic activity, although it is not clear if this is related to MMP inhibition; either way it may not be disadvantageous in a cancer therapeutic.<sup>41</sup> Notably, series 1 was overall of similar cytotoxic activity to the non-nitrates, although there were potentially important differences in individual pairs. For example, the piperazine nitrate **1c** was cytotoxic but its non-nitrate analogue **2c** was not. Also the dinitrate **1a**, which exerted profound effects on both MMPs, was not cytotoxic but its non-nitrate counterpart was ( $\text{CC}_{50}$ : 8.2/6.8  $\mu\text{M}$  in Caco-2/HT1080).

The MTT assay results with HT1080 cells suggested that some of the reduction in supernatant MMP-2 and MMP-9 observed previously was due to effects on cell viability. However, if it was merely a cytotoxic effect, then the reduction in the two enzyme levels should have been similar; instead, we observed that MMP-9 activity in the supernatant was more strongly affected than MMP-2 activity (Figure 3). Moreover, **1a** and **1e**, which were not especially cytotoxic ( $\text{CC}_{50}$  72.0, 78.7  $\mu\text{M}$ ), nevertheless exerted significant inhibitory effects on MMP-9 expression (38, 92%). We next sought to separate the cytotoxic effects from those on gelatinase secretion on the assumption that these were independent properties. The effect of series 1 on cell viability was therefore further characterized at 10  $\mu\text{M}$  using a flow cytometry approach to detect apoptotic (Annexin V) and necrotic cells (propidium iodide). Compounds **1a–f** did not increase apoptotic or necrotic populations

**Table 2.** Griess Assay Values for  $\text{NO}_2^-$  and  $\text{NO}_3^-$  Following Incubation of Series 1 at 200 and (10)  $\mu\text{M}$  over Caco-2 Monolayers for 24 h ( $n = 3$ )<sup>a</sup>

	<b>1a</b>	<b>1b</b>	<b>1c</b>	<b>1d</b>	<b>1e</b>	<b>1f</b>
$\text{NO}_x$	232.0 $\pm$ 14.1, (6.5 $\pm$ 1.3)	128.7 $\pm$ 8.8, (5.7 $\pm$ 0.7)	124.4 $\pm$ 4.2, (7.0 $\pm$ 0.9)	44.5 $\pm$ 10.8, (6.9 $\pm$ 1.6)	47.6 $\pm$ 10.1, (4.3 $\pm$ 0.9)	43.3 $\pm$ 12.0, (7.3 $\pm$ 0.9)
$\text{NO}_2^-$	164.3 $\pm$ 9.6	109.7 $\pm$ 19.9	46.5 $\pm$ 10.1	40.2 $\pm$ 15.1	30.7 $\pm$ 14.4	34.7 $\pm$ 11.8
$\text{NO}_3^-$	67.8 $\pm$ 12.9	18.9 $\pm$ 9.2	77.9 $\pm$ 3.4	4.3 $\pm$ 4.1	16.8 $\pm$ 11.6	8.6 $\pm$ 3.6

<sup>a</sup> $\text{NO}_x$  values represent the sum of  $\text{NO}_2^-$  and  $\text{NO}_3^-$ .

**Table 3. Effect of Compounds on Cell Viability (MTT) of Caco-2 and HT1080 Cells Expressed As CC<sub>50</sub> (Concentration Causing 50% Reduction in Cell Viability (95% Confidence Interval)) or % Inhibition of Viability at a Given Concentration Where There Was No Convergence with the Viability Data over a Concentration Range<sup>a</sup>**

	CC <sub>50</sub> (μM)			CC <sub>50</sub> (μM)	
	Caco-2	HT1080		Caco-2	HT1080
1a	>100 (6%, 100 μM)	72.0 (16.4–316.0)	2a	8.2 (6.4–10.4)	6.8 (5.5–8.4)
1b	>100 (28%, 100 μM)	48.5 (40.3–58.2)	2b	76.5 (44.6–131.2)	78.5 (61.3–100.4)
1c	26.0 (15.4–43.8)	12.8 (7.0–23.4)	2c	>100 (25%, 100 μM)	>100 (33%, 100 μM)
1d	>200 (100%, 200 μM)	78.7 (48.9–126.5)	2d	25.2 (19.8–32.0)	30.1 (26.1–34.7)
1e	>12.5 (12%, 2.5 μM)	11.8 (7.3–19.0)	2e	47.8 (37.8–60.6)	66.57 (55.85–79.3)
1f	>12.5 (37%, 12.5 μM)	8.1 (5.6–11.5)	2f	33.1 (27.4–40.0)	46.4 (29.6–72.5)

<sup>a</sup>CC<sub>50</sub> values were estimated from sigmoidal curves fitted to data across eight concentration levels, 0.1–200 μM (*n* = 3)

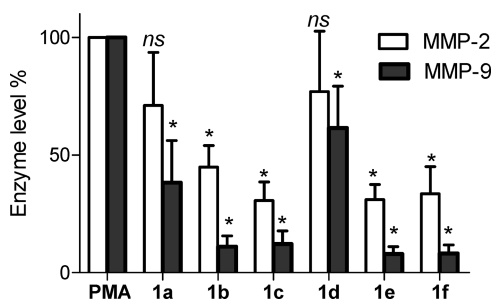


**Figure 3.** Zymographic analysis of MMP-2/MMP-9 activity from PMA (10 μM) stimulated HT1080 cell supernatants following treatment with 1a–f at 24 h at 100 μM showing large reductions in the activity of both enzymes.

following treatment of Caco-2 or HT1080 cells at 10 μM for 24 h (Supporting Information).

Thus, having validated a test concentration of 10 μM, the effect of series 1 and 2 on gelatinase secretion was assessed over 24 h using Caco-2 cells. We used this cell line because it had been less susceptible to loss of viability than the HT1080 cell line in the MTT assay. A mixture of IL1β/TNFα was used to stimulate cells in these experiments because this generates a more robust inflammatory response than PMA in Caco-2 cells. Series 1 and 2 were directly compared in an effort to exclude effects arising from their differences in potency/selectivity against the gelatinases or other MMPs (Figure 4). At 10 μM, all members of series 1 reduced MMP-9 secretion relative to control (*p* < 0.05). No effects were observed on MMP-2 levels. The nitrate compounds were consistently more efficacious inhibitors of MMP-9 secretion than series 2. These differences were significant in pairs 1b/2b, 1c/2c, and 1f/2f.

Because we had shown that the series 1 at 10 μM were capable of inhibiting cytokine-induced MMP-9 secretion, we repeated the tumor cell invasion assay at this higher concentration. We also increased the stimulus concentration (HGF (500 ng/mL) and PMA (10 μM)) in order to produce a stronger MMP-9 release and a more aggressively invasive cellular response. Under HGF stimulation, 1a significantly inhibited tumor cell invasion (51%) whereas its non-nitrate analogue 1b had no effect. The effects of the compounds on PMA induced invasion are presented in Figure 5. Nitrate analogues 1a, 1d, and 1e significantly inhibited cellular migration under PMA stimulation (43.3%, 44.5%, and 64.9%,

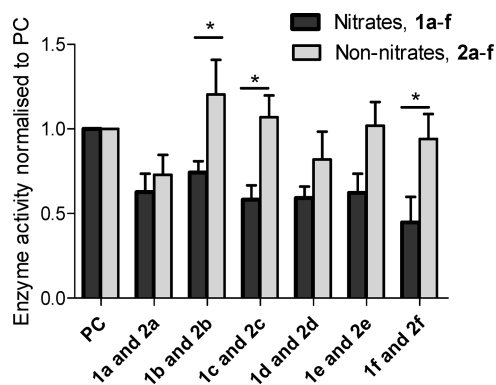


**Figure 4.** Normalized densitometry of MMP-9 gelatinolytic activity from supernatants of TNFα/IL1β (positive control (PC)) stimulated Caco-2 cell following treatment with 1a–f or 2a–f at 24 h at 10 μM. \**p* < 0.05.

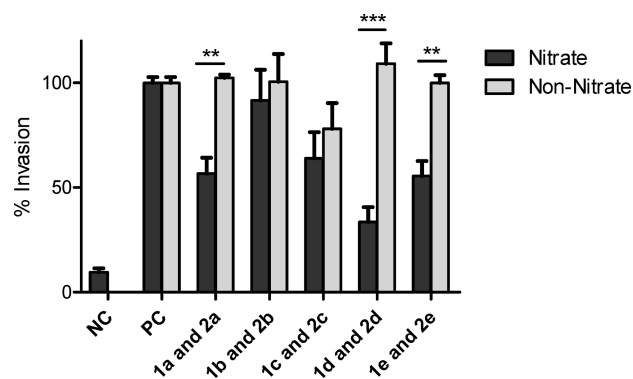


**Figure 5.** Caco-2 cell invasion through a matrigel membrane following stimulation with 10 μM PMA (positive control) and following incubation in the presence of nitrate/non nitrate pairs with 1a–e or 2a–e for 48 h. Values are normalized to positive control. *p* < 0.05 (Anova with Bonferroni Multiple Comparisons (sd, *n* = 3)).

respectively). The pair 1c/2c inhibited cell migration, but the effect was not significant. None of the non-nitrates significant affected cell invasion under these conditions.

## CONCLUSION

Several novel nitrate-substituted barbiturate-based gelatinase inhibitors were prepared maintaining a classical MMP P1'

phenoxyphenyl group at C5 but with a geminal P2' nitroxyalkyl amino group. The compounds retained intrinsic ability to inhibit gelatinase activity of recombinant human gelatinases but also liberated nitrite in a structure and concentration dependent manner. Compounds from series 1 inhibited MMP-9 secretion from Caco-2 cells stimulated with inflammatory cytokines, whereas their non-nitrate analogues did not. Nitrate compounds **1a**, **1d**, and **1e** (10  $\mu$ M) also inhibited tumor cell invasion in response to PMA, whereas their non-nitrate analogues did not. These interesting compounds merit further exploration of the interplay of NO and MMP-inhibitory factors. There is further scope within the general design for modulating inhibitory potency, selectivity, and NO donor/mimetic properties. The balance between inhibitory potency and NO-mediated anti-inflammatory effects will require study in appropriate disease models.

## EXPERIMENTAL SECTION

All chemicals were purchased from Sigma-Aldrich (Ireland), except where stated. All reactions were monitored using TLC. Uncorrected melting points were measured on a Stuart Apparatus. Infrared (IR) spectra were acquired on a Perkin-Elmer FT-IR Paragon 1000 spectrometer.  $^1\text{H}$  and  $^{13}\text{C}$  nuclear magnetic resonance (NMR) spectra were recorded at 27  $^\circ\text{C}$  on a Bruker DPX 400 spectrometer (400.13 MHz,  $^1\text{H}$ ; 100.61 MHz,  $^{13}\text{C}$ ). Coupling constants are reported in hertz. Electrospray ionization mass spectrometry (ESI-MS) was performed in the positive ion mode on a liquid chromatography time-of-flight mass spectrometer (Micromass LCT, Waters Ltd., Manchester, UK). The samples were introduced into the ion source by an LC system (Waters Alliance 2795, Waters Corporation, USA) in acetonitrile:water (60:40% v/v) at 200  $\mu\text{L}/\text{min}$ . The capillary voltage of the mass spectrometer was at 3 kV. The sample cone (declustering) voltage was set at 40 V. For exact mass determination, the instrument was externally calibrated for the mass range  $m/z$  100 to  $m/z$  1000. A lock (reference) mass ( $m/z$  556.2771) was used. Mass measurement accuracies of  $\pm 5$  ppm were obtained. RPHPLC was used to establish compound purity. The stationary phase was a Waters Xbridge C18, 5  $\mu\text{m}$  column (4.6 mm  $\times$  150 mm); the mobile phase consisted of a mixture of methanol and water (60:40) at a flow rate of 1 mL/min. HPLC was performed using a system consisting of a Waters 600 pump and controller, Waters 717 autosampler and a Waters 996 photodiode array detector controlled by Waters Empower Software. Chromatograms were extracted at 230 nm. All test compounds were >95% pure.

**General Synthetic Method.** A solution of 5-bromo-5-(4-phenoxyphenyl)pyrimidine-2,4,6(1H,3H,5H)-trione (**3**) in MeOH was treated with the appropriate alkyl amine (1.5 equiv) and  $\text{Et}_3\text{N}$  (3 equiv) at room temperature for 24 h. The solvents were evaporated and the products separated directly using flash chromatography.

**5-(4-Phenoxyphenyl)-5-(bis-(2-nitrooxy-ethyl)-amino)pyrimidine-2,4,6(1H,3H,5H)-trione (1a).** Product obtained as off-white solids (194 mg, 39.6%); mp 184–186  $^\circ\text{C}$ . HRMS:  $\text{C}_{20}\text{H}_{19}\text{N}_5\text{O}_{10}$  [ $\text{M} + \text{Na}^+$ ] requires 512.1182; found 512.1168.  $^1\text{H}$  NMR  $\delta$  (MeOH- $d_4$ ) ppm: 2.84–2.87 (t,  $J = 5.02$ , 4H), 4.64–4.67 (t,  $J = 5.02$ , 4H), 6.91–7.01 (m, 4H), 7.12–7.15 (t,  $J = 7.53$ , 1H), 7.34–7.38 (t,  $J = 7.53$ , 3H), 7.46–7.51 (m, 3H).  $^{13}\text{C}$  NMR  $\delta$  (MeOH- $d_4$ ) ppm: 46.7, 72.0, 100.8, 119.3, 120.6, 122.2, 125.2, 128.7, 131.1, 150.6, 157.6, 160.2, 170.5. IR (KBr)  $\nu$  ( $\text{cm}^{-1}$ ): 3068, 1728, 1706, 1648, 1281, 849.

**5-(4-Phenoxyphenyl)-5-(methyl-(2-nitrooxy-ethyl)-amino)pyrimidine-2,4,6(1H,3H,5H)-trione (1b).** Product was obtained as off-white solids (134 mg, 32.3%); mp 143–145  $^\circ\text{C}$ .  $\text{C}_{19}\text{H}_{18}\text{N}_4\text{O}_7$  [ $\text{M} + \text{Na}^+$ ] requires 437.1073; found 437.1078.  $^1\text{H}$  NMR  $\delta$  ( $\text{CDCl}_3$ ) ppm: 2.41 (s, 3H), 2.91–2.96 (m, 2H), 4.37–4.42 (m, 2H), 6.90–6.92 (d,  $J = 8.03$ , 2H), 7.00–7.02 (d,  $J = 8.03$ , 1H), 7.15–7.18 (t,  $J = 7.53$ , 1H), 7.34–7.38 (t,  $J = 7.53$ , 1H), 7.40–7.46 (m, 3H).  $^{13}\text{C}$  NMR  $\delta$  ( $\text{CDCl}_3$ ) ppm: 38.2, 49.8, 70.8, 100.8, 118.3, 119.8, 121.4, 124.6, 129.5, 130.0, 150.8, 155.6, 159.1, 171.2. IR (KBr)  $\nu$  ( $\text{cm}^{-1}$ ): 3066, 1720, 1698, 1644, 1280, 842.

**5-(4-Phenoxyphenyl)-5-(4-(2-nitrooxy-ethyl)piperazin-1-yl)pyrimidine-2,4,6(1H,3H,5H)-trione (1c).** Product was obtained as off-white solids (197 mg, 42.0%); mp 206–208  $^\circ\text{C}$ . HRMS:  $\text{C}_{22}\text{H}_{24}\text{N}_5\text{O}_7$  requires 470.1676; found 470.1679.  $^1\text{H}$  NMR  $\delta$  (DMSO- $d_6$ ) ppm: 2.47–2.51 (m, 6H), 2.62–2.68 (m, 4H), 4.05–4.08 (m, 2H), 7.02–7.07 (m, 4H), 7.17–7.21 (t,  $J = 7.53$ , 1H), 7.40–7.43 (m, 4H).  $^{13}\text{C}$  NMR  $\delta$  (DMSO- $d_6$ ) ppm: 47.8, 52.8, 57.3, 71.0, 74.0, 118.2, 118.4, 119.2, 121.4, 124.2, 129.6, 130.2, 150.2, 155.9, 159.3, 170.1. IR (KBr)  $\nu$  ( $\text{cm}^{-1}$ ): 3066, 1710, 1684, 1640, 1281, 849.

**5-(4-Phenoxyphenyl)-5-(4-(1-nitrooxy-ethyl)piperidin-1-yl)pyrimidine-2,4,6(1H,3H,5H)-trione (1d).** Product was obtained as off-white solids (158 mg, 34.8%); mp 190–192  $^\circ\text{C}$ . HRMS:  $\text{C}_{22}\text{H}_{23}\text{N}_4\text{O}_7$  requires 455.1561; found 455.1567.  $^1\text{H}$  NMR  $\delta$  ( $\text{CDCl}_3$ ) ppm: 1.16–1.27 (m, 2H), 1.47–1.58 (m, 3H), 2.32–2.37 (m, 2H), 2.77–2.83 (m, 2H), 4.84–4.90 (m, 2H), 6.92–6.95 (d,  $J = 8.53$ , 1H), 6.97–6.99 (d,  $J = 8.53$ , 2H), 7.01–7.03 (d,  $J = 8.53$ , 1H), 7.15–7.18 (t,  $J = 7.53$ ), 7.37–7.40 (t,  $J = 7.53$ , 1H), 7.43–7.48 (m, 3H).  $^{13}\text{C}$  NMR  $\delta$  ( $\text{CDCl}_3$ ) ppm: 27.4, 34.2, 49.1, 75.7, 76.1, 118.4, 119.8, 121.3, 124.3, 129.6, 130.2, 150.7, 155.9, 159.4, 170.6. IR (KBr)  $\nu$  ( $\text{cm}^{-1}$ ): 3068, 1732, 1694, 1642, 1286, 849.

**5-(4-Phenoxyphenyl)-5-(4-(2-nitrooxy-ethyl)piperidin-1-yl)pyrimidine-2,4,6(1H,3H,5H)-trione (1e).** Product was obtained as off-white solids (145 mg, 30.9%); mp 201–203  $^\circ\text{C}$ . HRMS:  $\text{C}_{23}\text{H}_{25}\text{N}_4\text{O}_7$  requires 469.1723; found (M + H) $^+$  = 469.1723.  $^1\text{H}$  NMR  $\delta$  ( $\text{CDCl}_3$ ) ppm: 1.33–1.39 (m, 2H), 1.42–1.46 (m, 2H), 1.48–1.51 (m, 1H), 1.73–1.78 (m, 2H), 2.57–2.64 (m, 2H), 2.76–2.79 (m, 2H), 4.78–4.82 (m, 2H), 6.92–6.94 (d,  $J = 8.53$ , 1H), 6.96–6.98 (d,  $J = 8.53$ , 2H), 7.03–7.05 (d,  $J = 8.53$ , 1H), 7.16–7.19 (t,  $J = 7.53$ , 1H), 7.36–7.40 (t,  $J = 7.53$ , 1H), 7.45–7.49 (m, 3H), 8.99 (s, 2H).  $^{13}\text{C}$  NMR  $\delta$  ( $\text{CDCl}_3$ ) ppm: 21.4, 32.2, 32.6, 48.1, 70.5, 76.0, 118.2, 119.7, 121.2, 124.2, 129.5, 129.9, 148.7, 155.8, 158.1, 169.8. IR (KBr)  $\nu$  ( $\text{cm}^{-1}$ ): 3068, 1732, 1704, 1633, 1285, 849.

**5-(4-Phenoxyphenyl)-5-(3-(1-nitrooxy-methyl)piperidin-1-yl)pyrimidine-2,4,6(1H,3H,5H)-trione (1f).** Product was obtained as off-white solids (181 mg, 39.8%); mp 190–192  $^\circ\text{C}$ . HRMS:  $\text{C}_{22}\text{H}_{23}\text{N}_4\text{O}_7$  requires 455.1568; found 455.1567.  $^1\text{H}$  NMR  $\delta$  ( $\text{CDCl}_3$ ) ppm: 1.28–1.30 (m, 1H), 1.3–1.40 (m, 1H), 1.56–1.59 (m, 1H), 1.64–1.68 (m, 1H), 1.71–1.76 (m, 1H, CH), 2.08–2.13 (m, 1H), 2.51–2.57 (m, 1H), 2.61–2.68 (m, 1H), 2.71–2.75 (m, 1H), 4.37–4.41 (m, 1H), 4.52–4.57 (m, 1H), 6.92–6.94 (d,  $J = 8.53$ , 1H), 6.96–6.99 (d,  $J = 8.53$ , 1H), 7.04–7.06 (d,  $J = 8.53$ , 1H), 7.16–7.20 (t,  $J = 7.53$ , 1H), 7.36–7.40 (t,  $J = 7.53$ , 2H), 7.45–7.49 (m, 2H), 9.15 (s, 1H), 9.16 (s, 1H).  $^{13}\text{C}$  NMR  $\delta$  ( $\text{CDCl}_3$ ) ppm: 26.6, 34.2, 48.8, 50.7, 53.7, 73.7, 74.6, 118.5, 119.7, 121.3, 124.2, 129.4, 129.9, 148.9, 155.7, 158.9, 170.0. IR (KBr)  $\nu$  ( $\text{cm}^{-1}$ ): 3066, 1723, 1688, 1640, 1281, 853.

**Biological Methods. Cell Culture and Treatment.** Human fibrosarcoma HT-1080 cells were cultured in Eagle's Minimal Essential Medium (MEM) containing 10% fetal bovine serum (FBS), 100 IU/mL penicillin, and 50  $\mu\text{g}/\text{mL}$  streptomycin. The cultures were incubated at 37  $^\circ\text{C}$  in a humidified 5%  $\text{CO}_2$  atmosphere until confluence. Caco-2 cells were cultivated in Eagle's minimal essential medium (MEM) containing 20% fetal bovine serum (FBS), 100 IU/mL penicillin, and 50  $\mu\text{g}/\text{mL}$  streptomycin.

**Zymography.** HT1080 cells were grown in 25 mL tissue culture flasks until approximately 75% confluent. The media was then changed to serum-free media, and the cells were treated with test compounds (100  $\mu\text{M}$ ) and incubated for 3 h. PMA (10  $\mu\text{M}$ ) was then added, and the flasks were incubated for 24 h at 37  $^\circ\text{C}$  in a humidified 5%  $\text{CO}_2$  atmosphere. The compounds were introduced in DMSO such that the final concentration did not exceed 0.1% DMSO. After 24 h, the supernatant was removed and centrifuged at 13000 rpm for 5 min to remove dead cells or floating debris. Supernatants were stored at  $-80$   $^\circ\text{C}$  until analysis. Caco-2 cells were grown in 25 mL tissue culture flasks in 20% FBS media until approximately 75% confluent. The media was then changed to serum-free, and the cells were then treated with test compounds at 100 nM or 10  $\mu\text{M}$  and incubated for 30 min. Cytokines TNF- $\alpha$  and IL-1 $\beta$  were then added at 10 ng/mL, and the flasks were incubated for 24 h at 37  $^\circ\text{C}$  in a humidified 5%  $\text{CO}_2$  atmosphere. The compounds were dissolved in DMSO to give a final



DMSO concentration of <1%. At 24 h, the conditioned media were collected and centrifuged at 13000 rpm for 5 min at RT to remove any dead cells or floating debris. The resultant supernatants were stored at  $-80^{\circ}\text{C}$  until analysis. Samples were normalized with respect to protein content using a Bradford assay. The enzymatic activities of MMP-2 and MMP-9 were assayed by gelatin zymography in serum-free media. The samples were electrophoresed on an SDS-PAGE containing 2% gelatin. The gels were washed with 2.5% Triton X three times for 20 min cycles. The gels were then washed twice and finally incubated with zymography buffer (0.15 M NaCl, 5 mM  $\text{CaCl}_2$ , 0.05%  $\text{NaN}_3$ , and 50 mM Tris-HCl buffer, pH 7.5) at  $37^{\circ}\text{C}$  for 48 h. After incubation, the gels were stained with 0.025% Coomassie Brilliant Blue G250 in 25% MeOH, 10% acetic acid, and  $\text{H}_2\text{O}$  and destained with acetic acid 8%, methanol 4%, and  $\text{H}_2\text{O}$ . The gelatinolytic activity was detected as a band of gelatin digestion and was quantified by densitometry using gel documentation system r (Bio-RAD, Universal hood II and Quantity One 4.6 software) and expressed as a percentage of the positive control (HT-1080 cells incubated with serum free media and cytokines in the absence of inhibitors).

**MMP-2 and MMP-9 Fluorogenic Assay.** Recombinant proMMP-2 and proMMP-9 (R&D Systems, Ireland) were activated by treatment with *p*-aminophenylmercuric acetate at  $37^{\circ}\text{C}$  for 1 and 24 h, respectively. The synthetic broad-spectrum fluorogenic substrate (7-methoxycoumarin-4-yl)-acetyl-pro-Leu-Gly-Leu-(3-(2,4-dinitrophenyl)-L-2,3-diaminopropionyl)-Ala-Arg-NH<sub>2</sub> (R&D Systems, UK) was used to assay MMP-2 and MMP-9 activity, as described.<sup>26</sup>

**Invasion Assay.** The BD BioCoat Matrigel Invasion Chamber assay system was used to study the pharmacological effects of the nitrates and alcohols on tumor cell migration. Briefly, the assay utilizes an invasion chamber consisting of a tissue culture plate with cell culture inserts and an 8  $\mu\text{m}$  pore size polycarbonate membrane. The upper surface of the insert membrane is coated with a thin layer of Matrigel Basement Membrane Matrix. Matrigel is an extract of basement membrane derived from a murine tumor, with identical components, both chemically and immunologically, to authentic basement membrane. The layer occludes the pores of the membrane, blocking noninvasive cells from migrating through the pores. Invasive cells, on the other hand, are able to degrade the matrix proteins that occlude the pores and this ability allows them to pass through the pores. The invasion assay was performed according to the manufacturer's instructions. Briefly, aliquots of 0.5 mL of cell suspensions consisting of  $2 \times 10^5$  Caco-2 cells/mL were added to the inserts and allowed to invade for 48 h in a humidified tissue culture incubator, at  $37^{\circ}\text{C}$ , 5%  $\text{CO}_2$  atmosphere. The tumor cells were stimulated with either PMA (10  $\mu\text{M}$ ) or HGF (100 ng/mL or 500 ng/mL). The noninvading cells were afterward removed by scrubbing with a cotton tipped swab and the cells on the lower surface of the membrane stained with Diff-Quik stain. The membrane was then examined by light microscopy using an Olympus CKX41 microscope (Olympus America Inc., Melville, NY, USA). Photomicrographs were captured using a digital camera and MicroFire (Olympus America Inc.) software. All the experiments were carried out in duplicate.

**MTT Assay.** Cell viability was determined by MTT assay. Cells were seeded (Caco-2 at  $8 \times 10^3$  cells/well and HT1080 at  $12 \times 10^4$  cells/well) into 96-well plates and grown until 70% confluent. Cells were serum starved for 1 h and then treated with test compounds at 0.1–200  $\mu\text{M}$  under serum-free conditions for 24 h. At the end of this incubation, MTT (0.5 mg/mL) was added and incubated for 3 h at  $37^{\circ}\text{C}$ . After 3 h, supernatants were removed, 100  $\mu\text{L}$  of DMSO was added, and the plates were incubated with shaking for 10 min. The formazan crystals formed inside the viable cells were solubilized in DMSO, and the optical density was read on a plate reader at 540 nm. The % cell viability was determined as follows: (optical density of treated cells/optical density of nontreated cells)  $\times$  100. The experiments were performed a minimum of three times with three replicates per concentration.

**Annexin V Flow Cytometry Assay.** Cells were grown to 80% confluence in T25 flasks and treated with test compounds for 24 h in serum-free medium; control cells were treated only with vehicle in serum-free media for 24 h. Following 24 h treatment, cells were

removed from T25 flasks and washed with  $10\times$  binding buffer (0.1 M HEPES (pH 7.4), 1.4 M NaCl, 25 mM  $\text{CaCl}_2$ ) before being resuspended in 100 mL of  $1\times$  binding buffer. A 20 mL aliquot of these cells was stained using 5 mL of Annexin V-FITC and 5 mL of propidium iodide and incubated at room temperature for 15 min in the dark. Following incubation, samples were diluted in  $1\times$  binding buffer and analyzed within 5 min using a BD FACSArray (BD Biosciences, Oxford, UK). Flow cytometry was performed on double-stained cell samples (Caco-2 and HT1080 cells). The instrument was set up to measure the size (forward scatter), granularity (side scatter), and cell fluorescence. Antibody binding was measured by analyzing individual cells for fluorescence. Data were analyzed using BD FACS Array software and expressed as a percentage of control fluorescence in arbitrary units.

**Griess Assay.** A series of nitrite and nitrate standard solutions were prepared with sodium nitrite and sodium nitrate from 3 to 200  $\mu\text{M}$ . A 200  $\mu\text{L}$  aliquot of each nitrite standard solution and 200  $\mu\text{L}$  of water was added to a 96-well plate.<sup>42</sup> For nitrate standard solutions, 200  $\mu\text{L}$  of  $4^{\circ}\text{C}$  saturated solution of  $\text{VCl}_3$  was added instead of water. The blank wells contained only 400  $\mu\text{L}$  of water. All the wells were treated at  $4^{\circ}\text{C}$  with 100  $\mu\text{L}$  of sulfanilamide (2% w/v) and 100  $\mu\text{L}$  of *N*-1-naphthylethylenediamine dihydrochloride (0.1 w/v). The plate was shaken for 45 min, and the absorbance was measured at 540 nm. The supernatants of the barbiturate-based nitrate treated Caco-2 cells following PMA stimulation (10  $\mu\text{M}$ ) were tested in similar manner. The resulting absorbance values of the supernatants were applied to the calibration line formula. The blank cellular data was generated by treating the cells with PMA in the absence of test article.

**Molecular Modeling.** The structure of MMP-9 (PDB code 2VOX) used was an MMP-9 active site mutant with barbiturate inhibitor. The barbiturate inhibitor and water molecules were removed. Docking calculations were carried out using AutoDock version 4.0 with the Lamarckian genetic algorithm (LGA). The molecular models of each inhibitor were built using the builder function of MOE and minimized with MOPAC 7 (AM1 method) interfaced to MOE. The Zn parameters were changed to zinc radius, 0.87 Å; well depth, 0.35 kcal/mol; and Zn atomic charge, +0.95. The 3D affinity grid box was designed to include the full active site and possible residues. The setting of the center of grid boxes was based on the value of active Zn. Docking calculations were set to 20 runs. Then 25000000 energy evaluations were allowed as a maximum in each run. At the end of the calculation, AutoDock performed cluster analysis. Docking solutions with ligand all-atom root-mean-square deviation (rmsd) within 2.0 Å of each other were clustered together and ranked by the lowest energy representative.

**Statistical Analysis.** All data are presented as group of means with standard error of the mean of  $n \geq 3$ . Statistical analysis of the mean difference between multiple groups was determined by one-way ANOVA followed by Tukey–Kramer multiple comparison post test. A *P* value <0.05 was considered to be statistically significant. All statistical analyses were performed using Prism version 4 for Windows, GraphPad Software, La Jolla, California, USA.

## ■ ASSOCIATED CONTENT

### 📄 Supporting Information

Synthesis and characterization data for compounds 2a–f; flow cytometry analysis of apoptosis in Caco-2 and HT1080 cells. This material is available free of charge via the Internet at <http://pubs.acs.org>.

## ■ AUTHOR INFORMATION

### Corresponding Author

\*Phone: +353-1-896 2795. Fax: +353-1-896 2793. E-mail: [gilmerjf@tcd.ie](mailto:gilmerjf@tcd.ie).

## ACKNOWLEDGMENTS

This work was supported in part by a Science Foundation of Ireland (SFI) Research Frontiers grant (RFP/BMT2781) awarded to C.M. C.M. is SFI Stokes lecturer.

## ABBREVIATIONS USED

AP-1, activator protein 1; annexin V FTC, annexin V fluorescein conjugate; DETA-NO, diethylenetriamine NON-Oate; FBS, fetal bovine serum; HRMS, high resolution mass spectrometry; HGF, hepatic growth factor; HPLC, high performance liquid chromatography; IL-1 $\beta$ , interleukin-1 $\beta$ ; IL-2, interleukin-2; IL-8, interleukin-8; MTP-1, membrane type matrix metalloproteinase-1; MTT, 3-(4,5-dimethylthiazol-2-yl)-2,5-diphenyltetrazolium bromide assay; NF $\kappa$ B, nuclear factor  $\kappa$ B; PK/PD, pharmacokinetic/pharmacodynamic; PMA, phorbolmyristate acetate; TNF- $\alpha$ , tumor necrosis factor- $\alpha$

## REFERENCES

- (1) Clark, I. M.; Swigler, T. E.; Sampieri, C. L.; Edwards, D. R. The regulation of matrix metalloproteinases and their inhibitors. *Int. J. Biochem. Cell Biol.* **2008**, *40*, 1362–1378.
- (2) Malemud, C. J. Matrix metalloproteinases (MMPs) in health and disease: an overview. *Front. Biosci.* **2006**, *11*, 1696–1701.
- (3) Brew, K.; Nagase, H. The tissue inhibitors of metalloproteinases (TIMPs): an ancient family with structural and functional diversity. *Biochim. Biophys. Acta* **1803**, 55–71.
- (4) Olson, M. W.; Toth, M.; Gervasi, D. C.; Sado, Y.; Ninomiya, Y.; Fridman, R. High affinity binding of latent matrix metalloproteinase-9 to the  $\alpha$ 2(IV) chain of collagen IV. *J. Biol. Chem.* **1998**, *273*, 10672–10681.
- (5) Back, M.; Ketelhuth, D. F.; Agewall, S. Matrix metalloproteinases in atherothrombosis. *Prog. Cardiovasc. Dis.* **2010**, *52*, 410–428.
- (6) (a) Gialeli, C.; Theocharis, A. D.; Karamanos, N. K. Roles of matrix metalloproteinases in cancer progression and their pharmacological targeting. *FEBS J.* **2011**, *278*, 16–27. (b) Rudek, M. A.; Venitz, J.; Figg, W. D. Matrix metalloproteinase inhibitors: do they have a place in anticancer therapy? *Pharmacotherapy* **2002**, *22*, 705–720.
- (7) Medina, C.; Radomski, M. W. Role of matrix metalloproteinases in intestinal inflammation. *J. Pharmacol. Exp. Ther.* **2006**, *318*, 933–938.
- (8) Naito, Y.; Yoshikawa, T. Role of matrix metalloproteinases in inflammatory bowel disease. *Mol. Aspects Med.* **2005**, *26*, 379–390.
- (9) Martin, M. D.; Matrisian, L. M. The other side of MMPs: protective roles in tumor progression. *Cancer Metastasis Rev.* **2007**, *26*, 717–724.
- (10) Chakraborti, S.; Mandal, M.; Das, S.; Mandal, A.; Chakraborti, T. Regulation of matrix metalloproteinases: an overview. *Mol. Cell. Biochem.* **2003**, *253*, 269–285.
- (11) Gum, R.; Lengyel, E.; Juarez, J.; Chen, J. H.; Sato, H.; Seiki, M.; Boyd, D. Stimulation of 92-kDa gelatinase B promoter activity by ras is mitogen-activated protein kinase 1-independent and requires multiple transcription factor binding sites including closely spaced PEA3/ets and AP-1 sequences. *J. Biol. Chem.* **1996**, *271*, 10672–10680.
- (12) Simon, C.; Simon, M.; Vucelic, G.; Hicks, M. J.; Plinkert, P. K.; Koitschev, A.; Zenner, H. P. The p38 SAPK pathway regulates the expression of the MMP-9 collagenase via AP-1-dependent promoter activation. *Exp. Cell Res.* **2001**, *271*, 344–355.
- (13) Zhao, X.; Benveniste, E. N. Transcriptional activation of human matrix metalloproteinase-9 gene expression by multiple co-activators. *J. Mol. Biol.* **2008**, *383*, 945–956.
- (14) Balasubramanian, S.; Fan, M.; Messmer-Blust, A. F.; Yang, C. H.; Trendel, J. A.; Jeyaratnam, J. A.; Pfeiffer, L. M.; Vestal, D. J. The interferon-gamma-induced GTPase, mGBP-2, inhibits tumor necrosis factor alpha (TNF-alpha) induction of matrix metalloproteinase-9 (MMP-9) by inhibiting NF-kappaB and Rac protein. *J. Biol. Chem.* **2011**, *286*, 20054–20064.

(15) Li, W.; Li, H.; Bocking, A. D.; Challis, J. R. Tumor necrosis factor stimulates matrix metalloproteinase 9 secretion from cultured human chorionic trophoblast cells through TNF receptor 1 signaling to IKK $\beta$ -NF $\kappa$ B and MAPK1/3 pathway. *Biol. Reprod.* **2010**, *83*, 481–487.

(16) Marshall, H. E.; Stamler, J. S. Inhibition of NF-kappa B by S-nitrosylation. *Biochemistry* **2001**, *40*, 1688–1693.

(17) Pfeilschifter, J.; Eberhardt, W. Molecular mechanisms of nitric oxide-dependent inhibition of TPA-induced matrix metalloproteinase-9 (MMP-9) in MCF-7 cells. *J. Cell Physiol.* **2009**, *219*, 276–287.

(18) Shin, C. Y.; Lee, W. J.; Choi, J. W.; Choi, M. S.; Ryu, J. R.; Oh, S. J.; Cheong, J. H.; Choi, E. Y.; Ko, K. H. Down-regulation of matrix metalloproteinase-9 expression by nitric oxide in lipopolysaccharide-stimulated rat primary astrocytes. *Nitric Oxide* **2007**, *16*, 425–432.

(19) Akool, el-S.; Kleinert, H.; Hamada, F. M.; Abdelwahab, M. H.; Förstermann, U.; Pfeilschifter, J.; Eberhardt, W. Nitric oxide increases the decay of matrix metalloproteinase 9 mRNA by inhibiting the expression of mRNA-stabilizing factor HuR. *Mol. Cell. Biol.* **2003**, *23*, 4901–4916.

(20) Ridnour, L. A.; Windhausen, A. N.; Isenberg, J. S.; Yeung, N.; Thomas, D. D.; Vitek, M. P.; Roberts, D. D.; Wink, D. A. Nitric oxide regulates matrix metalloproteinase-9 activity by guanylyl-cyclase-dependent and -independent pathways. *Proc. Natl. Acad. Sci. U.S.A.* **2007**, *104*, 16898–16903.

(21) McCarthy, S. M.; Bove, P. F.; Matthews, D. E.; Akaike, T.; van der Vliet, A. Nitric oxide regulation of MMP-9 activation and its relationship to modifications of the cysteine switch. *Biochemistry* **2008**, *47*, 5832–5840.

(22) Martelli, A.; Rapposelli, S.; Calderone, V. NO-releasing hybrids of cardiovascular drugs. *Curr. Med. Chem.* **2006**, *13*, 609–625.

(23) Jones, M.; Inkiewicz, I.; Medina, C.; Santos-Martinez, M. J.; Radomski, A.; Radomski, M. W.; Lally, M. N.; Moriarty, L. M.; Gaynor, J.; Carolan, C. G.; Khan, D.; O'Byrne, P.; Harmon, S.; Holland, V.; Clancy, J. M.; Gilmer, J. F. Isosorbide-based aspirin prodrugs: integration of nitric oxide releasing groups. *J. Med. Chem.* **2009**, *52*, 6588–6598.

(24) (a) Thatcher, G. R.; Bennett, B. M.; Reynolds, J. N. NO chimeras as therapeutic agents in Alzheimer's disease. *Curr. Alzheimer Res.* **2006**, *3*, 237–245. (b) Boschi, D.; Tron, G. C.; Lazzarato, L.; Chegaev, K.; Cena, C.; Di Stilo, A.; Giorgis, M.; Bertinaria, M.; Fruttero, R.; Gasco, A. NO-donor phenols: a new class of products endowed with antioxidant and vasodilator properties. *J. Med. Chem.* **2006**, *49*, 2886–2897. (c) Abdellatif, K. R.; Chowdhury, M. A.; Velázquez, C. A.; Huang, Z.; Dong, Y.; Das, D.; Yu, G.; Suresh, M. R.; Knaus, E. E. Celecoxib prodrugs possessing a diazen-1-ium-1,2-diolate nitric oxide donor moiety: synthesis, biological evaluation and nitric oxide release studies. *Bioorg. Med. Chem. Lett.* **2010**, *20*, 4544–4549. (d)

(25) Schnitzer, T. J.; Kivitz, A.; Frayssinet, H.; Duquesroix, B. Efficacy and safety of naproxen in the treatment of patients with osteoarthritis of the knee: a 13-week prospective, randomized, multicenter study. *Osteoarthritis Cartilage* **2010**, *18*, 629–639.

(26) Grams, F.; Brandstetter, H.; D'Alò, S.; Geppert, D.; Krell, H. W.; Leinert, H.; Livi, V.; Menta, E.; Oliva, A.; Zimmermann, G. Pyrimidine-2,4,6-triones: a new effective and selective class of matrix metalloproteinase inhibitors. *Biol. Chem.* **2001**, *382*, 1277–1285.

(27) Wang, J.; Medina, C.; Radomski, M. W.; Gilmer, J. F. N-Substituted homopiperazine barbiturates as gelatinase inhibitors. *Bioorg. Med. Chem.* **2011**, *19*, 4985–4999.

(28) Breyholz, H. J.; Schäfers, M.; Wagner, S.; Hölte, C.; Faust, A.; Rabeneck, H.; Levkau, B.; Schober, O.; Kopka, K. C-5-disubstituted barbiturates as potential molecular probes for noninvasive matrix metalloproteinase imaging. *J. Med. Chem.* **2005**, *48*, 3400–3409.

(29) Breyholz, H. J.; Wagner, S.; Faust, A.; Riemann, B.; Hölte, C.; Hermann, S.; Schober, O.; Schäfers, M.; Kopka, K. Radiofluorinated pyrimidine-2,4,6-triones as molecular probes for noninvasive MMP-targeted imaging. *ChemMedChem* **2010**, *5*, 777–789.

(30) Tochowicz, A.; Maskos, K.; Huber, R.; Oltenfreiter, R.; Dive, V.; Yiotakis, A.; Zanda, M.; Pourmotabbed, T.; Bode, W.; Goettig, P.



Crystal structures of MMP-9 complexes with five inhibitors: contribution of the flexible Arg424 side-chain to selectivity. *J. Mol. Biol.* **2007**, *371*, 989–1006.

(31) Gilmer, J. F.; Moriarty, L. M.; Clancy, J. M. Evaluation of nitrate-substituted pseudocholine esters of aspirin as potential nitro-aspirins. *Bioorg. Med. Chem. Lett.* **2007**, *17*, 3217–3220.

(32) (a) Keefer, L. K. Fifty Years of Diazeniumdiolate Research. From Laboratory Curiosity to Broad-Spectrum Biomedical Advances. *ACS Chem. Biol.* **2011**, *6*, 1147–1155. (b) Buonsanti, M. F.; Bertinaria, M.; Stilo, A. D.; Cena, C.; Fruttero, R.; Gasco, A. Nitric oxide donor beta2-agonists: furoxan derivatives containing the fenoterol moiety and related furazans. *J. Med. Chem.* **2007**, *50*, 5003–5011.

(33) Sugita, H.; Kaneki, M.; Furuhashi, S.; Hirota, M.; Takamori, H.; Baba, H. Nitric oxide inhibits the proliferation and invasion of pancreatic cancer cells through degradation of insulin receptor substrate-1 protein. *Mol. Cancer Res.* **2010**, *8*, 1152–1163.

(34) Daiber, A.; Wenzel, P.; Oelze, M.; Munzel, T. New insights into bioactivation of organic nitrates, nitrate tolerance and cross-tolerance. *Clin. Res. Cardiol.* **2008**, *97*, 12–20.

(35) (a) Schuhmacher, S.; Schulz, E.; Oelze, M.; König, A.; Roegler, C.; Lange, K.; Sydow, L.; Kawamoto, T.; Wenzel, P.; Münzel, T.; Lehmann, J.; Daiber, A. A new class of organic nitrates: investigations on bioactivation, tolerance and cross-tolerance phenomena. *Br. J. Pharmacol.* **2009**, *158*, 510–520. (b) Roegler, C.; König, A.; Glusa, E.; Lehmann, J. A novel class of nitrovasodilators: potency and in vitro tolerance of organic aminoalkyl nitrates. *J. Cardiovasc. Pharmacol.* **2010**, *56*, 484–490.

(36) Oelze, M.; Knorr, M.; Schell, R.; Kamuf, J.; Pautz, A.; Art, J.; Wenzel, P.; Münzel, T.; Kleinert, H.; Daiber, A. Regulation of human mitochondrial aldehyde dehydrogenase (ALDH-2) activity by electrophiles in vitro. *J. Biol. Chem.* **2011**, *286*, 8893–8900.

(37) Schiefer, I. T.; Abdul-Hay, S.; Wang, H.; Vanni, M.; Qin, Z.; Thatcher, G. R. Inhibition of amyloidogenesis by nonsteroidal anti-inflammatory drugs and their hybrid nitrates. *J. Med. Chem.* **2011**, *54*, 2293–2306.

(38) Dos Santos, J. L.; Lanaro, C.; Lima, L. M.; Gambero, S.; Franco-Penteado, C. F.; Alexandre-Moreira, M. S.; Wade, M.; Yerigenahally, S.; Kutlar, A.; Meiler, S. E.; Costa, F. F.; Chung, M. Design, synthesis, and pharmacological evaluation of novel hybrid compounds to treat sickle cell disease symptoms. *J. Med. Chem.* **2011**, *54*, 5811–5819.

(39) Wagner, D. A.; Glogowski, J.; Skipper, P. L.; Wishnok, J. S.; Tannenbaum, S. R. Analysis of nitrate, nitrite, and [<sup>15</sup>N]nitrate in biological fluids. *Anal. Biochem.* **1982**, *126*, 131–138.

(40) Sato, H.; Takino, T. Coordinate action of membrane-type matrix metalloproteinase-1 (MT1-MMP) and MMP-2 enhances pericellular proteolysis and invasion. *Cancer Sci.* **2010**, *101*, 843–847.

(41) Rossello, A.; Nuti, E.; Catalani, M. P.; Carelli, P.; Orlandini, E.; Rapposelli, S.; Tuccinardi, T.; Atkinson, S. J.; Murphy, G.; Balsamo, A. A new development of matrix metalloproteinase inhibitors: twin hydroxamic acids as potent inhibitors of MMPs. *Bioorg. Med. Chem. Lett.* **2005**, *15*, 2311–2314.

(42) Miranda, K. M.; Espey, M. G.; Wink, D. A. A rapid, simple spectrophotometric method for simultaneous detection of nitrate and nitrite. *Nitric Oxide* **2001**, *5*, 62–71.